Journal of the Korean Ceramic Society
Vol. 47, No. 2, pp. 199~204, 2010.

DOI:10.4191/KCERS.2010.47.2.199

Fabrication of a $MnCo_2O_4$/gadolinia-doped Ceria (GDC) Dual-phase Composite Membrane for Oxygen Separation

Eun Jeong Yi, Mi Young Yoon, Ji-Woong Moon*, and Hae Jin Hwang†

School of Materials Science and Engineering, Inha University, Incheon 402-751, Korea
**Research Institute of Industrial Science & Technology, Pohang 790-330, Korea*

(Received February 16, 2010; Revised February 20, 2010; Accepted February 22, 2010)

ABSTRACT

A dual-phase ceramic membrane consisting of gadolinium-doped ceria (GDC) as an oxygen ion conducting phase and $MnCo_2O_4$ as an electron conducting phase was fabricated by sintering a GDC and $MnCo_2O_4$ powder mixture. The $MnCo_2O_4$ was found to maintain its spinel structure at temperatures lower than 1200°C. (Mn,Co)(Mn,Co)O_4 spinel, manganese and cobalt oxides formed in the sample sintered at 1300°C in an air atmosphere. XRD analysis revealed that no reaction phases occurred between GDC and $MnCo_2O_4$ at 1200°C. The electrical conductivity did not exhibit a linear relationship with the $MnCo_2O_4$ content in the composite membranes, in accordance with percolation theory. It increased when more than 15 vol% of $MnCo_2O_4$ was added. The oxygen permeation fluxes of the composite membranes increased with increasing $MnCo_2O_4$ content and this can be explained by the increase in electrical conductivity. However, the oxygen permeation flux of the composite membranes appeared to be governed not only by electrical conductivity, but also by the microstructure, such as the grain size of the GDC matrix.

Key words **: *Oxygen separation, Perovskite, $MnCo_2O_4$, GDC, Composite***

1. Introduction

Dense ceramic membranes with ionic and electronic conductivity, such as those composed of perovskite oxides, can be used for high-temperature oxygen separation and catalytic reactions, such as the partial oxidation of methane. They can separate oxygen selectively from air if an oxygen pressure difference is applied across the membrane. Oxygen is reduced to oxygen ions on the high-oxygen pressure side, which diffuse through the membrane and are oxidized to oxygen molecules on the low-oxygen pressure side. When hydrocarbons such as methane are supplied on the low-oxygen pressure side, they react with oxygen to produce hydrogen and carbon monoxide. This unique behavior originates from the presence of oxygen vacancies and free electrons in the crystal structure of the mixed ionic and electronic conducting (MIEC) oxide. Among the various oxides, $SrCo_{0.8}Fe_{0.2}O_{3-\delta}$ (SCF), $La_{1-x}Sr_xCo_{1-y}Fe_yO_{3-\delta}$ (LSCF) and $Ba_{0.5}Sr_{0.5}Co_{0.8}Fe_{0.2}O_{3-\delta}$ (BSCF) perovskites are the most famous and have been widely investigated by many researchers.[1-3]

In general, oxygen permeation flux across the membrane depends not only on its conductivity, or so-called ambipolar conductivity ($\sigma_{el} \cdot \sigma_{ion}/\sigma_{el}+\sigma_{ion}$), but also on its geometry, i.e., the thickness of the membrane.[4,5] Thus, the membrane should be as thin as possible. This requires the membrane to be tough, especially at high temperatures. However, perovskite-type MIEC oxides do not have high strength and toughness and suffer from low structural stability at high temperatures.[6] A thin film perovskite membrane, which is coated on a mechanically tough and chemically inert support, i.e., a bi-layer type membrane, might serve as an alternative.[7] However, it may also have some problems, such as cracking, delamination, etc., which are derived from the thermal expansion mismatch between the support and thin film.

A dual-phase composite membrane can usually be fabricated by incorporating an electronic conducting phase into an ionic conducting matrix. The advantages of dual-phase composites over single-phase, mixed ionic-electronic conductors are their chemical stability, compatibility with other membrane components, and mechanical stability.[8,9] YSZ/Pd,[10] $Bi_{1.5}Y_{0.3}Sm_{0.2}O_3$ (BYS)/Ag,[11] erbia-stabilized bismuth oxide (BE)/noble metal,[8] and $La_{0.2}Sr_{0.8}CoO_{3-\delta}$ (Pd/Ag)[12] are typical examples of dual-phase composite membranes. Recently, spinel- or perovskite-type electronic conducting oxide particles-dispersed dual-phase composite membranes were reported by Kagomiya et al.[13,14] and Li et al.,[15] respectively.

In this work, Gd-doped ceria ($Gd_{0.1}Ce_{0.9}O_2$, GDC) was used as an ionic conductor and $MnCo_2O_4$ as an electronic conductor. Generally, spinels containing manganese and cobalt are known to have the highest electrical conductivity and the largest degree of non-stoichiometry because of their multiple valence states.[16] In addition, $MnCo_2O_4$ is stable at high temperature, is easier to sinter than other spinel-type oxides, and has a low thermal expansion coefficient. The

†Corresponding author : Hae Jin Hwang
E-mail : hjhwang@inha.ac.kr
Tel : +82-32-860-7521 Fax : +82-32-862-4482

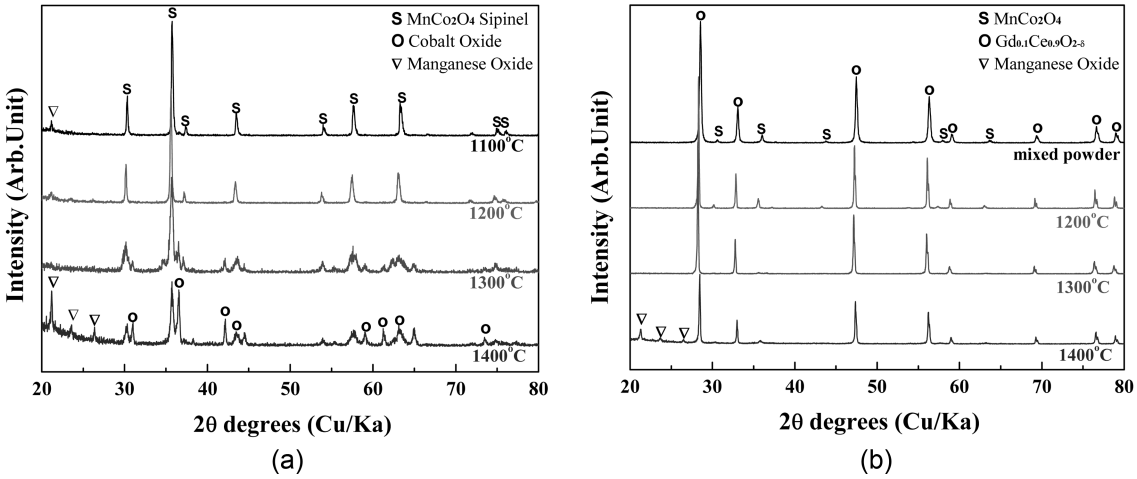

Fig. 1. XRD patterns of the $MnCo_2O_4$ (a) and $MnCo_2O_4$/GDC composite membranes (b) sintered at various temperatures.

sintering behavior, electrical properties and oxygen permeation characteristics of the GDC/$MnCo_2O_4$ composite membrane were investigated.

2. Experimental Procedure

Commercially available $Gd_{0.1}Ce_{0.9}O_2$, (GDC, Aanan Kasei Co. Ltd., Japan) and $MnCo_2O_4$ powders, which were synthesized in-house using a conventional solid-state reaction method from MnO_2 (99%, Sigma Aldrich, USA) and Co_3O_4 (99%, High Purity Chemicals, Japan) were mixed using a planetary mill. The dried powder mixture was uniaxially pressed into disk or rectangular bar-type green compacts with a diameter of 25 mm and subsequently CIPed at 200 MPa. The green compacts were sintered at 1200 and 1300°C for 5 h in an air atmosphere. The heating rate was 5°C/min. The sintered membrane samples were then ground and polished using diamond slurries to a thickness of 0.5 mm for oxygen permeation measurement.

The crystalline phases of the powders and sintered membranes were determined by X-ray diffractometry (XRD) with CuKα radiation. The diffraction patterns were collected at room temperature in the range of $20° \le 2\theta \le 80°$. The bulk density was measured via the Archimedes method. The electrical conductivity of the sintered membranes was measured in a stagnant air atmosphere by a four-probe method in which a few milliamperes was applied to the two outer electrodes of a rectangular bar-type membrane sample and the resulting potential difference between the two inner electrodes was read using a high-accuracy multimeter. Pt wires were used as the electrodes. The surface microstructure was observed by field emission scanning electron microscopy (FESEM, HITACHI, S-4200, Japan).

Disk-type membrane samples, each 0.5 mm thick, were held in place by two alumina tubes and two Pyrex rings were inserted between the sample and the alumina tube. Pure oxygen was introduced into the upstream side of the membrane sample at a flow rate of 50 sccm. Argon gas was fed to the downstream side of the membrane at a flow rate of 50 sccm. Both the upstream and downstream sides were maintained at atmospheric pressure. The effluent gas from the downstream side was analyzed by micro gas chromatography (Micro-GC). If any nitrogen was found in the effluents by Micro-GC due to slight sealing imperfections, the corresponding leakage of oxygen was subtracted when calculating the oxygen permeation flux through the membrane. In addition, oxygen leakage through the membrane was checked by flowing nitrogen to the upstream side of the membrane before and after the oxygen permeation measurement.

3. Results and Discussion

Fig. 1 shows the XRD patterns of the $MnCo_2O_4$ and $MnCo_2O_4$/GDC composite membranes sintered at 1100, 1200, 1300 and 1400°C for 5 h. All of the peaks for the $MnCo_2O_4$ samples sintered at 1100 and 1200°C were assigned to a spinel phase. On the other hand, cobalt oxide and (Co, Mn)$(Mn,Co)_2O_4$, which is a non-stoichiometric spinel with a tetrahedral structure and octahedral sites occupied randomly by Co and Mn, were observed in the $MnCo_2O_4$ sample sintered at 1300°C. The relative peak intensity of CoO increased and manganese oxide peaks were also observed in the XRD pattern of the sample sintered at 1400°C. This result suggests that the $MnCo_2O_4$ phase is unstable at temperatures higher than 1200°C.

The $MnCo_2O_4$/GDC composite membranes exhibited similar phase evolution behavior to the $MnCo_2O_4$ sample. The peaks responsible for the $MnCo_2O_4$ spinel phase were clearly observed in the samples sintered at 1100 and 1200°C. It was found that all of the peaks corresponded to an $MnCo_2O_4$ or GDC phase and there were no extra peaks due to unwanted reactions between the two phases, suggesting that $MnCo_2O_4$ is the phase that is compatible with the GDC matrix at 1200°C. However, the relative peak intensity of $MnCo_2O_4$ decreased in the 1300°C-sintered sam-

Table 1. Bulk and Relative Densities of $MnCo_2O_4$/GDC Composites Membranes Sintered at Various Temperatures

Sintering temperature. (°C)	8 vol% $MnCo_2O_4$/GDC		15 vol% $MnCo_2O_4$/GDC		24 vol% $MnCo_2O_4$/GDC	
	bulk†	relative‡	bulk	relative	bulk	relative
1200	6.61	94.6	6.84	96.1	6.69	96.1
1300	6.75	97.5	6.60	96.0	6.59	95.6
1400	6.32	-	6.67	-	6.71	-

†g/cm^3
‡theoretical density: 7.102, 6.978 and 6.820 g/cm^3 for 8, 15 and 24 vol% $MnCo_2O_4$/GDC

ple and a manganese oxide phase appeared in the 1400°C-sintered sample.

Table 1 summarizes the bulk and relative densities of the $MnCo_2O_4$/GDC composite membranes sintered at various temperatures. It seems that there is no distinct relationship between the bulk density and the sintering temperature. The bulk density of the 8 vol% $MnCo_2O_4$/GDC composite membrane sintered at 1300°C was higher than that of the corresponding sample sintered at 1200°C and decreased slightly at 1400°C. On the other hand, the situation was different in the 24 vol% $MnCo_2O_4$/GDC composite membranes. This might be associated with the phase stability of the $MnCo_2O_4$ phase. As mentioned previously, the $MnCo_2O_4$ phase is not stable at temperatures higher than 1200°C and, thus the sintering behavior of the composite membrane might be complicated, depending on both the $MnCo_2O_4$ content and sintering temperature. In addition, since the melting temperature of $MnCo_2O_4$ lies between 1300 and 1400°C, depending on its atomic ratio of Mn and Co,[17] presumably the density anomaly is caused by the so-called swelling effect, which was reported by Takamura et al..[13]

Supposing that the theoretical densities of the 8, 15 and 24 vol% $MnCo_2O_4$/GDC composites are 7.10, 6.98 and 6.82 g/cm^3, respectively, the relative density of the membranes sintered at 1200°C can be estimated to be 94.6, 96.1 and 96.1%. This suggests that $MnCo_2O_4$ accelerated the sintering of the GDC matrix. In the case of the samples sintered at 1400°C, it is hard to evaluate their relative density because of their phase instability. However, it can be inferred that adding $MnCo_2O_4$ has a positive effect on the sinterability of the composite membrane.

Figs. 2 and 3 provide SEM photographs showing the typical microstructures of the $MnCo_2O_4$/GDC composite membranes sintered at 1200°C and 1300°C, respectively. $MnCo_2O_4$ particles, which have a somewhat irregular morphology, were homogeneously dispersed in the GDC matrix grains. For the 8 vol% $MnCo_2O_4$/GDC composite, $MnCo_2O_4$ existed as isolated particles, as can be seen in Fig. 2 (a) and Fig. 3 (a), while they began to connect to each other in the 15 vol% and formed a three-dimensional network structure in the 24 vol% $MnCo_2O_4$/GDC composite membrane. For the 1200°C-sintered samples, the grain size of the GDC matrix was estimated to be approximately 2~3 μm and it increased slightly as the $MnCo_2O_4$ content was increased. This result suggests that the $MnCo_2O_4$ particles did not act as a grain growth inhibitor during the sintering of the GDC matrix. The grain size of the GDC matrix increased with increasing temperature.

Generally, spinels with transition metals in their octahedral sites show high electrical conductivity and are known to conduct electrons or holes by a hopping mechanism. Of the various spinel-type materials, $MnCo_2O_4$ has an electri-

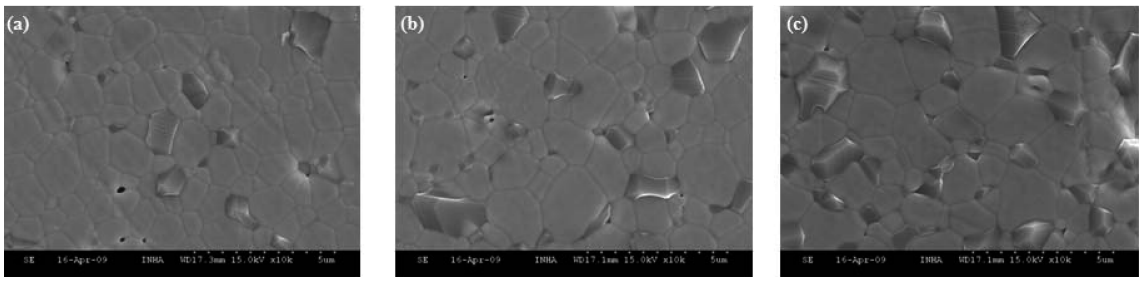

Fig. 2. SEM photographs of the $MnCo_2O_4$/GDC composite membranes sintered at 1200°C; (a) 8 vol% $MnCo_2O_4$ (b) 15 vol% $MnCo_2O_4$, (c) 24 vol% $MnCo_2O_4$.

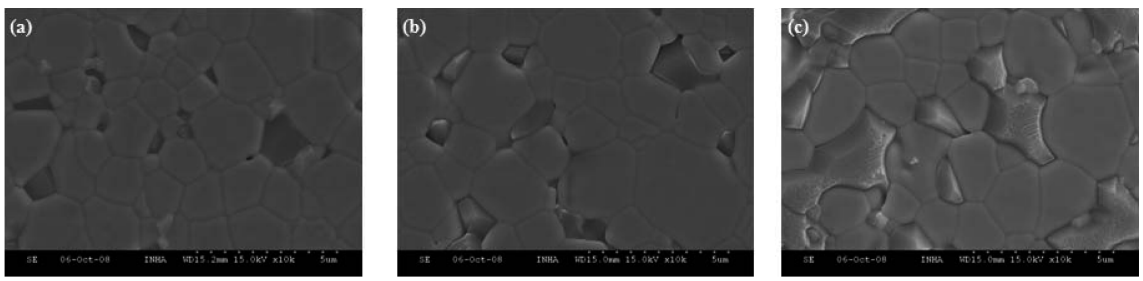

Fig. 3. SEM photographs of the $MnCo_2O_4$/GDC composite membranes sintered at 1300°C; (a) 8 vol% $MnCo_2O_4$ (b) 15 vol% $MnCo_2O_4$, (c) 24 vol% $MnCo_2O_4$.

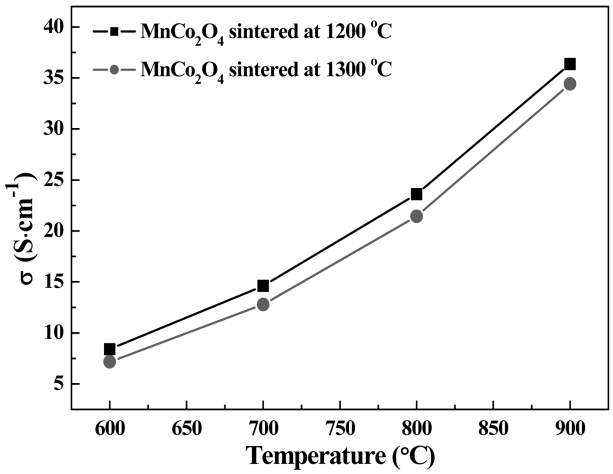

Fig. 4. Electrical conductivity of the $MnCo_2O_4$ samples sintered at 1200 and 1300°C as a function of temperature.

cal conductivity of over 100 S/cm at 900°C.[18] Fig. 4 shows the electrical conductivity of the $MnCo_2O_4$ samples sintered at 1200 and 1300°C as a function of temperature. The electrical conductivity increased with increasing temperature, indicating that the $MnCo_2O_4$ spinel shows a typical semiconductor- type conduction mechanism. The electrical conductivities of the $MnCo_2O_4$ samples were 7~8 and 34~36 S/cm at 600 and 900°C, respectively.

Fig. 5 shows the electrical conductivity of the $MnCo_2O_4$/GDC composite membranes as a function of the $MnCo_2O_4$ content. The electrical conductivity of the composite membranes was lower than that of the pure $MnCo_2O_4$ and higher than that of the GDC matrix (10^{-2} and 10^{-1} S/cm at 600°C and 900°C, respectively). The electrical conductivity of the 8 vol% $MnCo_2O_4$/GDC composite membrane was almost the same or slightly lower than that of the GDC matrix. This result suggests that adding less than 8 vol% of $MnCo_2O_4$ does not allow for the creation of electronic conduction paths, because the $MnCo_2O_4$ exists in the form of isolated particles. On the other hand, the electrical conductivity of the composite membranes containing more than 15 vol% of $MnCo_2O_4$ increased with increasing $MnCo_2O_4$ content. As can be seen in Figs. 2 and 3, the $MnCo_2O_4$ particles began to connect to each other at 15 vol% $MnCo_2O_4$ and formed a three-dimensional network at 24 vol% $MnCo_2O_4$. As the $MnCo_2O_4$ content increases, the connectivity of the particles was improved, thereby increasing the electrical conductivity.

Fig. 6 shows the oxygen permeation fluxes of the composite membranes sintered at 1200 and 1300°C. It is well

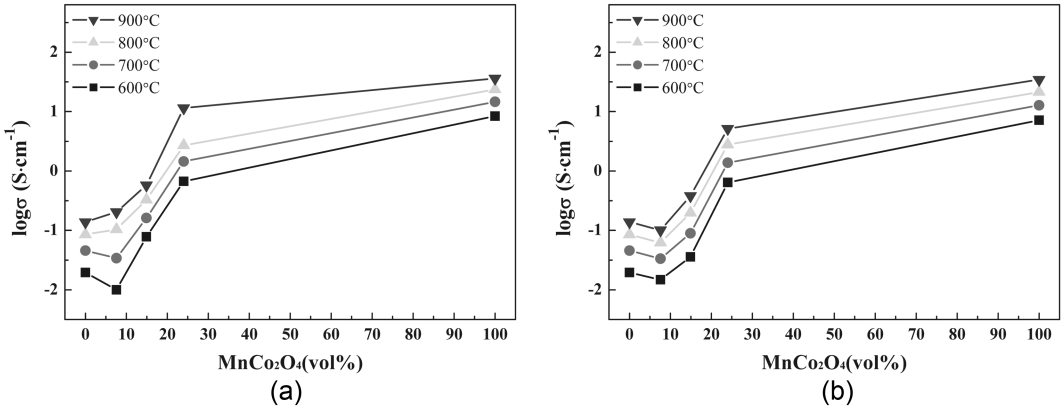

Fig. 5. Electrical conductivity of $MnCo_2O_4$/GDC composite membranes sintered at 1200 (a) and 1300°C (b).

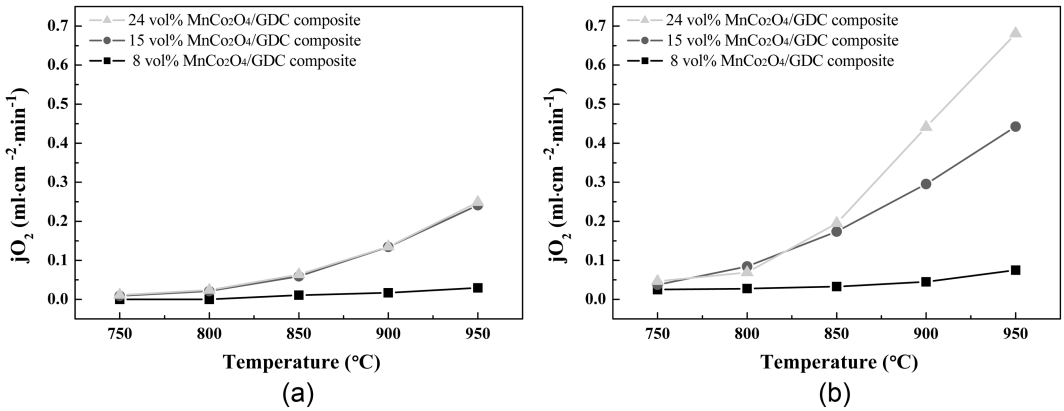

Fig. 6. Oxygen permeation flux of the $MnCO_2O_4$/GDC composite membranes sintered at 1200°C (a) and 1300°C (b) as a function of temperature.

known that GDC is a good oxygen ion conductor. Since the oxygen ion conductivity of $MnCo_2O_4$ is negligible, the oxygen ion transport through the $MnCo_2O_4$/GDC composite membrane is thought to be mainly via GDC matrix grains or grain boundaries. In addition, the connectivity of the $MnCo_2O_4$ phase is very important to produce an oxygen-permeable composite membrane, i.e., both GDC and $MnCo_2O_4$ phases should form three-dimensional network structures. It was found that the 8 vol% $MnCo_2O_4$/GDC composite membranes did not show any oxygen permeation in the temperature region of 750 to 950°C. This was due to the poor connectivity of the $MnCo_2O_4$ phase and the resulting low conductivity of the composite, as can be seen in Figs. 5 (a) and (b). In this study, it appears that the interconnection between $MnCo_2O_4$ particles started to form when 15 vol% $MnCo_2O_4$ was added to the GDC matrix. The 15 and 24 vol% $MnCo_2O_4$/GDC composite membranes exhibited oxygen permeability which increased with increasing temperature, because the oxygen ion diffusivity increased with increasing temperature. An interesting feature observed in Fig. 6 is that the composite membranes sintered at 1300°C exhibited a higher oxygen permeation flux than the composites sintered at 1200°C, although their electrical conductivities were almost the same, as is evident in Fig. 4.

The observed high oxygen permeability in the 1300°C-sintered composite membranes appeared to be closely related to the increase in the grain size, as can be seen in Figs. 2 and 3. The grain size of the 1300°C-sintered composite membranes was higher than that of the 1200°C-sintered ones. Since the grain boundaries served as an undesirable scattering center for the diffusion of oxygen ions, the oxygen permeation flux increased as the grain size of the membrane increased. Several researchers reported that an increase in the average grain size leads to increased oxygen permeation in MIEC materials. They explained this phenomenon in terms of the higher oxygen ion transport rate through the grain than through the grain boundaries.[19,20]

The oxygen permeation flux vs. $MnCo_2O_4$ content curves of the composite membranes sintered at 1200 and 1300°C are shown in Fig. 7. The oxygen permeation flux increases with increasing $MnCo_2O_4$ content. However, the increase in the oxygen permeation flux was remarkable in the 15 vol% $MnCo_2O_4$/GDC samples and modest in the 24 vol% $MnCo_2O_4$/GDC sample. This observed phenomenon is considered to be associated with the microstructure change and the resulting increase in the oxygen ion diffusivity. Generally, the oxygen permeation flux, jO_2, of a mixed ionic and electronic conducting (MIEC) material can be expressed in terms of its ionic conductivity, σ_i, electronic conductivity, σ_e, and oxygen partial pressure gradient using Wagner's formula, as follows:[21]

$$jO_2 = -\frac{RT}{16F^2L}\int_{\ln P(O_2)'}^{\ln P(O_2)''} \frac{\sigma_i\sigma_e}{\sigma_i+\sigma_e} d\ln P(O_2)$$

where R, F, T, and L are the gas constant, Faraday constant, temperature and membrane thickness, respectively. The oxygen permeation flux is proportional to ambipolar conductivity, i.e., $\sigma_i\sigma_e/(\sigma_i+\sigma_e)$, not ionic conductivity or electronic conductivity. In other words, the oxygen permeability of the membrane was limited by the lower of the two conductivities.

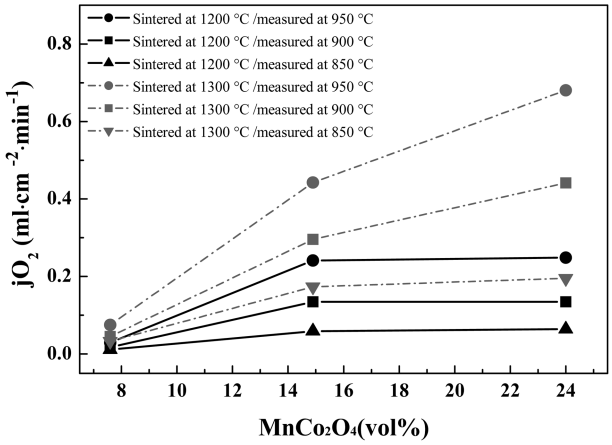

Fig. 7. Oxygen permeation flux of the $MnCO_2O_4$/GDC composite membranes sintered at 1200 and 1300°C as a function of the $MnCo_2O_4$ content.

The pure GDC and 8 vol% $MnCo_2O_4$/GDC composite membranes did not show any oxygen permeability, because of their low electronic conductivity. The increase in the electronic conductivity in the 15 vol% $MnCo_2O_4$ composite membrane was responsible for the increase in its oxygen permeation flux. The fact that the increase in the oxygen permeation flux in the 24 vol% $MnCo_2O_4$/GDC composite membrane sintered at 1200°C was modest means that its oxygen permeation was not limited by the electronic conductivity, i.e., the increase in the electronic conductivity in the 24 vol% $MnCo_2O_4$/GDC composite membrane did not contribute to the enhancement of the oxygen permeation flux.

4. Conclusion

Almost fully densified $MnCo_2O_4$/GDC composite membranes were fabricated at 1200 and 1300°C by a pressureless sintering technique from a GDC and $MnCo_2O_4$ powder mixture. The XRD analysis revealed that $MnCo_2O_4$ was compatible with the GDC matrix up to 1200°C. However, the $MnCo_2O_4$ spinel decomposed at temperatures above 1300°C, leading to the formation of tetragonal-type (Mn,Co)(Co,Mn)O_4, manganese and cobalt oxides. It was found that the electrical conductivity of the composite membranes depended on the connectivity of the $MnCo_2O_4$ particles. At $MnCo_2O_4$ contents of more than 15 vol%, electron conducting pathways started to form and the electrical conductivity of the composite increased with increasing $MnCo_2O_4$ content. The $MnCo_2O_4$/GDC composite membranes showed oxygen permeability in the temperature region of 800 to 950°C, irrespective of the content of $MnCo_2O_4$. The oxygen perme-

ation flux of the composite membranes was determined by their electrical conductivity and microstructure. It was considered that a high electrical conductivity (an enhanced connectivity between $MnCo_2O_4$ particles) and large grain size is beneficial to produce a composite membrane with high oxygen permeability.

Acknowledgments

This work was supported by the Korea Science and Engineering Foundation (KOSEF) grant funded by the Korea government (MEST) (No. 2009-0083658).

REFERENCES

1. Y. Teraoka, H. M. Zhang, S. Furukawa, and N. Yamazoe, "Oxygen Permeation Through Perovskite-type Oxides," *Chem. Lett.*, **14** 1743-46 (1985).
2. P. N. Dyer, R. E. Richards, S. L. Russek, and D. M. Taylor, "Ion Transport Membrane Technology for Oxygen Separation and Syngas Production," *Solid State Ionics*, **134** 21-33 (2000).
3. T. Ishihara, Y. Tsuruta, T. Todaka, H. Nishiguchi, and Y. Takita, "Fe Doped $LaGaO_3$ Perovskite Oxide as an Oxygen Separating Membrane for CH_4 Partial Oxidation," *Solid State Ionics,* **152** 709-14 (2002).
4. C. Wagner, "Theory of tarnishing process," *Z. Phys. Chem.*, **B21** 25-41 (1933).
5. K. Wiik, S. Aasland, H. L. Hansen, I. L. Tangen, and R. Odegard, "Oxygen Permeation in the System $SrFeO_{3-x}$-$SrCoO_{3-y}$," *Solid State Ionics*, **152-53** 675-80 (2002).
6. Y. Zeng and Y. S. Lin, "Stability and Surface Catalytic Properties of Fluorite-structured Yttria-doped Bismuth Oxide under Reducing Environment," *J. Catal.*, **182** 30-6 (1999).
7. O. Buchler, J. M. Serra, W. A. Meulenberg, D. Sebold, And H. P. Buchkremer, "Preparation and properties of thin $La_{1-x}Sr_xCo_{1-y}Fe_yO_{3-\delta}$ Perovskitic Membranes Supported on Tailored Ceramic Substrates," *Solid State Ionics*, **178** 90-9 (2007).
8. C. S. Chen, H. Kruidhof, H. J. M. Bouwmeester, H. Verweij, and A. J. Burggraaf, "Oxygen Permeation Through Oxygen Ion Oxide-noble Metal Dual Phase Composites," *Solid State Ionics*, **86-8** 569-72 (1996).
9. Z. Wu and M. Liu, "Modeling of Ambipolar Transport Properties of Composite Mixed Ionic-electronic Conductors," *Solid State Ionics*, **93** 65-84 (1997).
10. T. J. Mazanec, T. L. Cable, and J. G. Frye, "Electrocatalytic Cells for Chemical Reaction," *Solid State Ionics*, **53-6** 111-18 (1992).
11. J. Kim and Y. S. Lin, "Synthesis and Oxygen Permeation Properties of Ceramic-metal Dual-phase Membranes," *J. Membrane Sci.*, **167** 123-33 (2000).
12. Y. Y. Liu and L. Hong, "Fabrication and characterization of (Pd/Ag)-$La_{0.2}Sr_{0.8}CoO_{3-\delta}$ Composite Membrane on Porous Asymmetric Substrates," *J. Membrane Sci.*, **224** 137-50 (2003).
13. H. Takamura, T. Kobayashi, T. Kasahara, and A. Kamegawa, M. Okada, "Oxygen Permeation and Methane Reforming Properties of Ceria-based Composite Membranes," *J. Alloys and Compounds*, **408-12** 1084-89 (2006).
14. I. Kagomiya, T. Iijima, and H. Takamura, "Oxygen Permeability of Nanocrystalline $Ce_{0.8}Gd_{0.2}O_{1.9}$-$CoFe_2O_4$ Mixed-conductive Films," *J. Membrane Sci.*, **286** 180-84 (2006).
15. Q. Li, X. Zhu and W. Yang, "Single-step Fabrication of Asymmetric Dual-phase Composite Membranes for Oxygen Separation," *J. Membrane Sci.*, **325** 11-5 (2008).
16. E. Rios, J. -L. Gautier, G. Poillerat, and P. Chartier, "Mixed Valency Spinel Oxides of Transition Metals and Electrocatalysis: Case of the $Mn_xCo_{3-x}O_4$ System," *Electrochimica Acta*, **44** 1491-97 (1998).
17. E. Aukrust and A. Muan, "The Stabilities of $CoO \cdot Al_2O_3$, $CoO \cdot Cr_2O_3$, and $2CoO \cdot SiO_2$, *J. Am. Ceram. Soc.*, **46** 358-360 (1963).
18. A. Petric and H. Ling, "Electrical Conductivity and Thermal Expansion of Spinels at Elevated Temperatures," *J. Am. Ceram. Soc.*, **90** 1515-20 (2007).
19. V. V. Kharton, A. V. Kovalevsky, A. A. Taremchenko, F. M. Fiqueiredo, E. N. Naumovich, A. L. Shaulo, and F. M. B. Marques, "Surface Modification of $La_{0.3}Sr_{0.7}CoO_{3-\delta}$ Ceramic Membranes," *J. Membrane Sci.*, **195** 277-87 (2002).
20. V. V. Kharton , F. M. Fiqueiredo, A. V. Kovalevsky, A. P. Viskup, E. N. Naumovich, A. A. Yaremchenko, I.A. Bashmakov, and F. M. B. Marques, "Processing, Microstructure and Properties of $LaCoO_{3-\delta}$ Ceramics," *J. Euro. Ceram. Soc.*, **21** 2301-09 (2001).
21. Y. S. Lin, W. J. Wang, and J. H. Han, "Oxygen Permeation Through Thin Mixed-conducting Solid Oxide Membranes," *AIChE Journal*, **40** 786-98.